A Turn-on Fluorescent Probe for Detection of Sub-ppm Level Sulfur Mustard Simulant with High Selectivity

Yuanlin Zhang, Yanlin Lv, Xuefei Wang, Aidong Peng, Kaiquan Zhang, Xiaoke Jie, Jijun Huang, and Zhiyuan Tian

Anal. Chem., **Just Accepted Manuscript** • DOI: 10.1021/acs.analchem.8b01057 • Publication Date (Web): 12 Mar 2018

A Turn-on Fluorescent Probe for Detection of Sub-ppm Level Sulfur Mustard Simulant with High Selectivity

Yuanlin Zhang [a], Yanlin Lv [a], Xuefei Wang [a], Aidong Peng [b], Kaiquan Zhang [a], Xiaoke Jie [a], Jijun Huang [b,] and Zhiyuan Tian [a,]**

[a] School of Chemical Sciences, University of Chinese Academy of Sciences, Beijing 100049, P. R. China. E-mail: zytian@ucas.ac.cn

[b] College of Materials Science and Opto-Electronic Technology, University of Chinese Academy of Sciences, Beijing 100049, P. R. China. E-mail: jjh@ucas.ac.cn

ABSTRACT

A new type of fluorescent probe capable of detecting sulfur mustard (SM) simultant with concentration of 1.2 μM in solution and 0.5 ppm in gas phase has been developed. Owing to its molecular structure with thiocarbonyl component and two piperidyl moieties integrated into the xanthene molecular skeleton, this probe underwent a highly selective nucleophilic reaction with SM simultant and generated a thiopyronin derivative emitting intensive pink fluorescence. The distinct difference in electronic structure between the probe and thiopyronin derivative generated a marked shift of the absorbance band from 445 nm to 567 nm, which enabled an optimal wavelength propitious to excite the thiopyronin derivative but adverse to the probe. Such efficient separation of excitation wavelength and tremendous increase in fluorescence quantum yield, from less than 0.002 to 0.53, upon conversion from the probe to thiopyronin derivative jointly led to distinct contrast in the beaconing fluorescence signal (up to 850-fold) and therefore the unprecedented sensitivity for detecting SM species.

Sulfur mustard (bis(2-chloroethyl) sulfide, SM), a colorless to amber oily liquid with a garlic-like odor, is popularly known as mustard gas and was widely used as chemical war agent in World War I and many military conflicts thereafter, leading to millions of casualties.[1-3] Owing to its high toxicity and powerful ability to incapacitate opponents, SM was called the "king of war gases" and "chemical weapon of choice in modern tactical warfare".[4-6] Exposure to SM typically leads to dose-dependent skin injury even areas of necrosis, eye injuries even permanent blindness, respiratory failure even death.[7,8] Additionally, SM may be carcinogenic and mutagenic to human beings due to the chromosomal damage that it induced, especially for those undergoing long-term exposure.[9] It is known that SM molecule generates toxicity based on the spontaneous formation of a highly reactive and unstable sulfonium intermediate via an intramolecular cyclization.[10] Specifically, such cyclic intermediate is prone to react with a wide variety of biological molecules carrying electron-rich moieties such as sulphydryl (-SH) and amino ($-NH_2$) groups of tissue macromolecules (e.g. proteins and nucleic acids), resulting in chromatid aberrations and DNA strand breaks and apoptosis. Such acute damage, together with the rapid inactivation of sulphydryl-containing proteins and peptides such as glutathione, is expected to prevent cellular division and directly lead to programmed cell death. Alternatively, if cell death is not immediate, the chromosomal damage may siginificantly increase the incidence of malignancies for those suffered SM exposure.[11, 12]

It is particularly noteworthy that victims after the initial exposure to SM typically undergo a latent phase ranging from 30 min to 8 h before the development of toxic signs and symptoms.[13] Such intoxication latent phase of SM typically delays decontamination efforts and therefore leads to continued SM inhalation of victims suffered accidential exposure to SM. SM remains as a serious public health and safety threat, especually for civilians and soldiers in conflict zones, in

light of the virtual difficulty in verifying and controlling the manufacture or storage of SM and its highly toxic feature. What is even more worse is that there have been no effective antidotes for SM poisoning to date,[14] which unequivocally highlights the vital significance of strategies for promptly and reliably verifying trace amount of SM and the following emergency reponse. According to the acute exposure guideline levels (AEGLs) established for guiding emergency planning, prevention, and response in case of accidents or terrorist attacks with chemical agents, SM with concentration at or below AEGL-1 level, namely 0.06 ppm, does not cause observed adverse effects on health for general public subject to exposure duration of 10 min.[15,16] According to the Haber's rule for guaging the toxic effect of poisonous gas, a dose schema of 10-min exposure to 0.06 ppm poisonous gas is equivalent to acute exposure to 0.6 ppm gas with duration time of 1 minute. Thus, the first and primary point of focus in terms of minimizing the degree of SM injury shifts to reliable detection of trace amount of SM before its concentration reaches to such safety ceiling level.

A variety of strategies, including GC–MS,[17-22] ion mobility spectrometry,[23,24] quartz crystal microbalance analysis,[25] molecularly imprinted polymers,[26] platinum (II) pincer,[27] and immunochemical methods[28-30] have been reported for detection of SM. However, these strategies generally suffer from disadvantages including poor portability, complicated operation, low sensitivity and/or recognition selectivity. In contrast, fluorescence-based detection is highly advantageous regarding sensitivity, spatiotemporal resolution, and ease of manipulation.[31, 32] Based on a metal-ion indicator displacement mechanism, Anslyn et al. developed the first SM fluorescent probe with a detection limit of 0.2 mM for 2-chloroethyl ethyl sulfide (2-CEES),[33] an SM simulant that is chemically closely related to SM, known as "half mustard", but free from the associated toxicological properties.[11,34] To take a step further, Anslyn et al. developed another

type of probe for chromogenic and fluorometric detection of 2-CEES with a detection limit of 10 μM and the ability for gaseous SM sensing.[35] Pardasani and coworkers reported a rhodamine-based fluorescent probe enables detection of gaseous SM at a level of 6.25 ppm/30 min with naked eye.[36] Despite significant advancement on SM sensing, there is still a pressing need of fluorescent probes for promptly and reliably detecting SM with concentration below the AEGL-1 safety ceiling level for minimizing the degree of SM injury. As consistent efforts in pursuit of fluorescent probes for volatile hazardous chemicals sensing,[37] we developed a pyronin-based fluorescent probe capable of detecting SM with concentration down to 0.6 μM (in solution phase) and presenting huge contrast in beaconing fluorescence signal upon exposure to 0.25 ppm gaseous SM in this work. This is the first paradigm where a fluorescent probe enables facile and highly selective detetcion of SM with concentration indeed below the AEGL-1 safety ceiling level (Table S1 in the Supporting Information), which providing an effective modality for prompt detection of SM species in emergency events prior to the emergence of adverse effects on health of general public exerted by such toxic substance.

SM typically undergoes spontaneous first order intramolecular cyclization to form a hyperactive episulphonium cation intermediate, which readily reacts with and alkylates nucleophiles such as sulphydryl (-SH) and amino ($-NH_2$) groups of proteins and acids.[38] Benefiting from its large size and feature of easy polarization, sulfur atom is featured with easy accessibility of its unshared electron pair and therefore very suitable to act as the counterpart nucleophile.[39] On the other hand, thiols are prone to undergo oxidation in the presence of oxygen to form less ractive disulfide speices.[38] With these in mind, we constructed a sulfur-based fluorescent probe, 3, 6-di(piperidin-1-yl)-9H-xanthene-9-thione (DPXT), with thiocarbonyl component and two electron-donating piperidyl moieties integrated into the xanthene molecular

skeleton in this work. Specifically, the thiocarbonyl component is expected to avoid the undesirable S-S coupling of the probes while the 3, 6-position electron-donating piperidyl moieties augment the nucleophicility of sulfur, which greatly enhances the probe's reactivity in the SM-mediated nucleophilic reaction (**Scheme 1**).

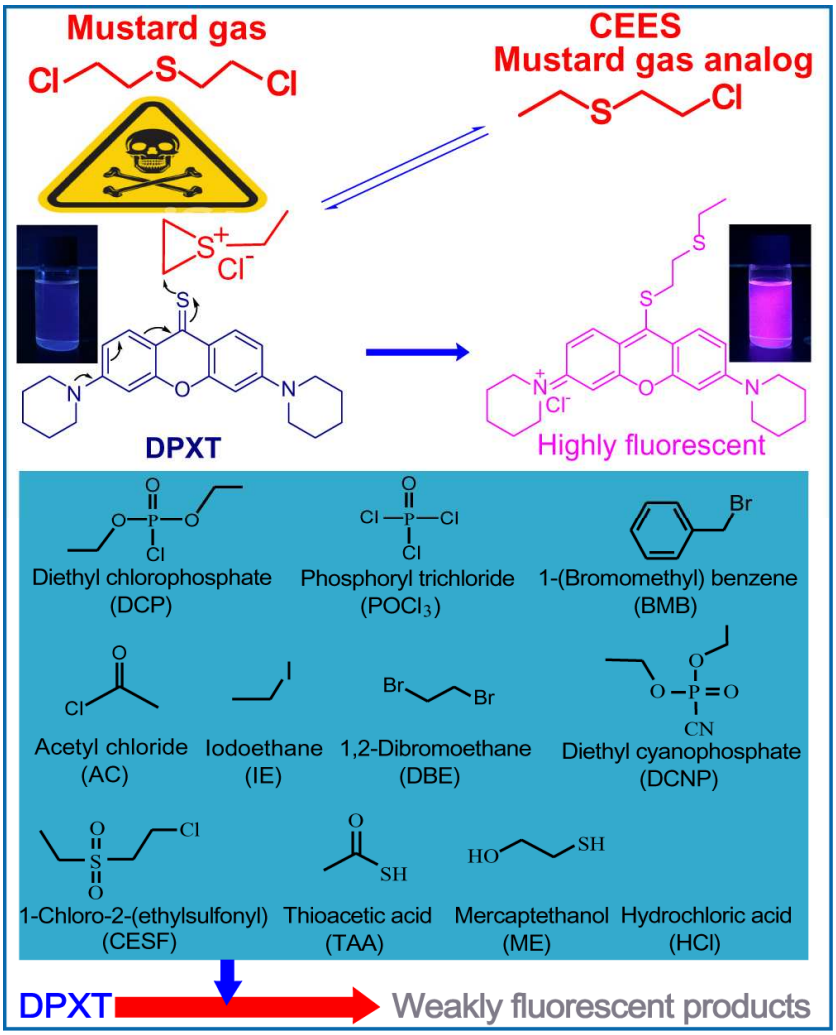

Scheme 1. Chemical structures of the fluorescent probe (DPXT) and analogues including representative acylating agents, alkylating agent, sulphur-containing compounds and hydrochloric acid investigated as interferent components and the proposed mechanism for 2-CEES sensing.

■ EXPERIMENTAL SECTION

Materials and Methods. *N*, *N*-dimethylformamide (DMF), dimethyl sulphoxide (DMSO), toluene, methanol, acetone, ethyl acetate (EA), acetonitrile, chloroform ($CHCl_3$), 1, 2-dichloroethane and dichloromethane (DCM) were purchased from Beijing Chemical Works (Beijing, China), and dried before used. All deuterium solvents used in the nuclear magnetic resonance spectroscopy (NMR) characterization were purchased from Sigma-Aldrich. Silica gel (200-300 mesh) for column chromatography was purchased from Qingdao Ocean Chemicals Inc. All other chemicals were purchased from J & K Scientific, Ltd., and used without further purification unless otherwise stated. NMR spectra were recorded in $CDCl_3$, or DMSO-d_6, or CD_2Cl_2 at ambient temperature on a Bruker Avance 300 or JEOL JNM-LA400. Matrix-assisted laser desorption ionization-time of flight (MALDI-TOF) mass spectra were recorded with a Bruker BIFLEX-III mass spectrometer. UV−vis absorption spectra were acquired on a UV-2550 spectrophotometer (Shimadzu, Japan). Steady-state fluorescence spectra were recorded on FluoroMax-4 spectrofluorometer (Horiba Jobin Yvon, NJ, USA).

Determination of the Fluorescence Quantum Yield. The fluorescence quantum yield of DPXT probe was estimated via the comparison of the integrated area of its corrected emission spectrum with that of a perylene/EtOH solution as a standard (ϕ = 0.92).[40] Likely, the fluorescence quantum yield of thiopyronin derivative was estimated using the solution of rhodamine B in EtOH solution as a standard (ϕ = 0.70).[41]

Determination of the Limit of Detection (LOD). The limit of detection was determined based on the method reported in the previous literature.[42] The fluorescence emission spectrum of DPXT in DCM was acquired 10 times and the standard deviation of blank measurement was achieved. Subsequently, a plot of the emission peak intensity (at 593 nm) against the

concentration of 2-CEES was obtained. The limit of detection was then determined based on the 3-sigma method.

Evaluation of Response of DPXT-loaded TLC Plate to Gaseous 2-CEES. A TLC plate was patterned with "CEES" logo using a DPXT/DCM stock solution (100 μM) and then placed in the air to evaporate the solvent. The photographs of TLC plate were firstly acquired under illumination of indoor light and a UV lamp (Ex. 365 nm), respectively. 50 μL of 2-CEES/DCM solution (1.1 mM) was added into a 2.5 L conical flask and then the lid was quickly closed. Gently heating the conical flask generated a specific sealed space filled with 0.5 ppm gaseous 2-CEES. The aforementioned TLC plate was put in such conical flask and then taken out 2 minutes later for the counterpart photographs acquisition, respectively. Six parallel TLC plates were loaded with DPXT by immersing one end of each plate in a DPXT/DCM stock solution (100 μM) and these plates were then placed in the air to evaporate the solvent. Subsequently, these DPXT-loaded TLC plates after 1-minute exposure to 2-CEES gas with concentration of 0, 0.5, 1.0, 1.5, 2.0, 2.5 ppm, respectively, were imaged under illumination of 365-nm light via the identical procedure.

Synthesis of 3, 6-Dihydroxy-9H-xanthen-9-one (2). 2, 2', 4, 4'-Tetrahydroxybenzophenone (Compound 1) (2.46 g, 10.0 mmol) in H_2O (40 ml) was heated at 200 °C for 6 h in a sealed tube. After cooling, the product was collected by filtration, washed with cold hexane and dried, affording 2 as a white solid (2.28 g, 10.0 mmol, 100%). ^{1}H NMR (400 MHz, d_6-DMSO): δ 6.81, (d, 2H, J = 2.2 Hz), 6.85 (dd, 2H, J = 8.8 Hz, 2.2 Hz), 7.98 (d, 2H, J = 8.8 Hz), 10.82 (s, 2H); ^{13}C NMR (100 MHz, d_6-DMSO): δ 102.15, 113.69, 114.18, 127.89, 157.64, 163.37, 174.13.

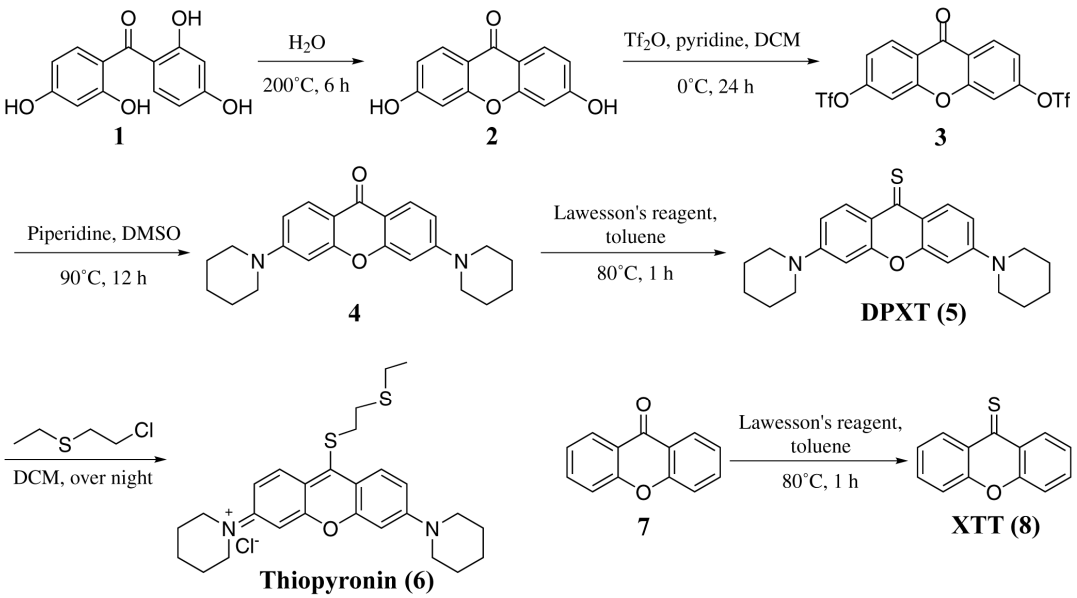

Scheme 2. Synthetic route to DPXT probe, thiopyronin derivative and reference compound XTT.

Synthesis of 3, 6-Ditriflatexanthone (3). 3, 6-Dihydroxyxanthone (2) (2.28 g, 10.0 mmol) was added to 300 ml DCM and pyridine (8.1 mL, 100 mmol). The resulting mixture was cooled to at 0 °C. Then Tf_2O (5.0 mL, 30.1 mmol) in CH_2Cl_2 was added dropwise. The reaction mixture was warmed to room temperature and stirred for 24 hr. The reaction was quenched with H_2O and the organic layer was washed with H_2O, 1 N HCl aq. and brine, and dried over Na_2SO_4. After evaporation, the residue was purified by flash chromatography on silica gel (DCM/petroleum ether =1 : 1) to give the target product (3.9 g, 7.9 mmol, 80%) as white needles. ^{1}H NMR (400 MHz, $CDCl_3$) δ 8.43 (d, 2H, J = 8.9 Hz), 7.47 (d, 2H, J = 2.3 Hz), 7.33 (dd, 2H, J = 8.9, 2.3 Hz); ^{13}C NMR(100 MHz, $CDCl_3$) δ 174.5, 156.6, 153.3, 129.6, 121.4, 118.7, 118.2, 111.4.

Synthesis of 3, 6-Di-piperidin-1-yl-xanthen-9-one (4). 3, 6-Ditriflatexanthone (3) (2.4 g, 5.0 mmol) was dissolved in 20 mL DMSO and piperidine (4.9 mL, 50.0 mmol) was added. The reaction mixture was heated to 90 °C and stirred for 12 h. The solution was cooled to room temperature and water was added. After treatment using water, the reaction mixture was poured

into DCM (100ml) and the organic layer was washed with H_2O, saturated Na_2CO_3 (aq.) and brine, and dried over Na_2SO_4. After evaporation, the residue was purified by flash chromatography on silica gel (DCM) to give the target product (1.6 g, 4.4 mmol, 90%) as yellow solid. ^{1}H NMR (300 MHz, d_6-DMSO) δ 7.86 (d, 2H, J = 9.0 Hz), 6.98 (dd, 2H, J = 9.0, 2.3 Hz), 6.74 (d, 2H, J = 2.3 Hz), 3.41 (br, 8H), 1.60 (br, 12H); ^{13}C NMR (75 MHz, d_6-DMSO) δ 173.0, 157.7, 154.8, 126.8, 111.7, 111.3, 98.8, 47.8, 24.8, 23.9. MALDI-MS: $[M+H]^+$ calcd for $C_{23}H_{26}N_2O_2$ 362.1944; found 363.2068.

Synthesis of 3, 6-Di (piperidin-1-yl)-9H-xanthene-9-thione (5). 3, 6-Di-piperidin-1-yl-xanthen-9-one (4) (0.34 g, 1.0 mmol) was dissolved in 20 mL toluene. Lawesson's Reagent (0.41 g, 1.0 mmol) was added. The reaction mixture was heated to 80 °C and stirred for 1 h. The solution was cooled to room temperature and water was added. After treatment using water, the reaction mixture was poured into ethyl acetate (50ml) and the organic layer was washed with H_2O and brine, and dried over Na_2SO_4. After evaporation, the residue was purified by flash chromatography on silica gel (DCM) to give the target product (0.22 g, 0.58 mmol, 58%) as red solid. ^{1}H NMR ($CDCl_3$, 400 MHz): δ8.66(s, 1H), 8.64(s, 1H) 6.92(d, J =4.0 Hz, 1H), 6.89(d, J =4.0 Hz, 1H), 6.61(s, 1H), 3.45 (m, *8*H), 1.70 (m, 12H) ppm; ^{13}C NMR ($CDCl_3$, 100 MHz): δ196.30, 155.3, 153.2, 131.7, 120.82, 98.21, 48.58, 25.4, 24.6 ppm; MALDI-MS: $[M+H]^+$ calcd for $C_{11}H_{12}BF_2N_3H^+$: 378.1766, Found: 379.1879.

Synthesis of Thiopyronin (6). 3, 6-di (piperidin-1-yl)-9H-xanthene-9-thione (5) (0.19 g, 0.5 mmol) was dissolved in 10 mL DCM. 2-Chloroethyl ethyl sulfide (5.8 mL, 50.0 mmol) was added. The reaction mixture was stirred for overnight. After evaporation, the residue was purified by flash chromatography on silica gel (DCM/MeOH=95:5) to give the target product (0.20 g, 0.40 mmol, 80%) as red solid. ^{1}H NMR ($CDCl_3$, 400 MHz): δ8.26 (s, 1H), 8.23(s, 1H)

7.23(s, 2H), 6.96 (s, 1H), 3.77 (m, 8H), 3.36 (t, 2H), 2.74 (t, 2H) , 1.79 (m, 12H), 1.19 (t, 3H) ppm; ^{13}C NMR (DMSO-d_6, 150 MHz): δ157.13, 156.70, 156.52, 131.73, 115.69, 97.13, 49.05, 38.90, 31.91, 26.28, 25.36, 24.22, 15.21 ppm; MALDI-MS: $[M]^+$ calcd for $C_{11}H_{12}BF_2N_3^+$: 467.2185, Found: 467.2186.

Synthesis of xanthene-9-thione (8). Xanthone (Compound 7) (0.20 g, 1.0 mmol) was dissolved in 10 mL toluene. Lawesson's Reagent (0.41 g, 1.0 mmol) was added and then the reaction mixture was heated to 80 °C and stirred for 1 h. The solution was cooled to room temperature and water was added. After treatment using water, the reaction mixture was poured into ethyl acetate (50ml) and the organic layer was washed with H_2O and brine, and dried over Na_2SO_4. After evaporation, the residue was purified by flash chromatography on silica gel (petroleum ether/DCM=5:1) to give the target product (0.19 g, 0.90 mmol, 90%) as dark green solid. ^{1}H NMR (400 MHz, $CDCl_3$): δ8.76-8.73 (m, 2H), 7.78-7.74 (m, 2H), 7.51-7.49 (m, 2H), 7.40-7.35 (m, 2H); ^{13}C NMR (100 MHz, $CDCl_3$): 205.21, 150.55, 134.98, 129.93, 129.08, 124.83, 118.35; MALDI-MS: $[M]^+$ calcd for $C_{13}H_8OS^+$: 212.0, Found: 211.8.

■ RESULTS AND DISCUSSION

Optical Response of DPXT to 2-CEES. As illustrated in Figure 1, DPXT probe in CH_2Cl_2 (DCM) solution clearly displayed UV-vis absorption and fluorescence emission spectra highly dependent on 2-CEES species. Specifically, the DPXT/DCM solution sample with pale yellow color presented intense absorption feature in the range of 400-485 nm with maximum at ~445 nm. Upon addition of small aliquots of 2-CEES to the sample, a new absorption band in the region of 480-640 nm with peak ~ 576 nm and a shoulder at ~530 nm, respectively, clearly emerged. Additionally, such new absorption band was found gradually augment accompanying with the concomitant decrease of the short-wavelength absorption band upon further incremental

addition of 2-CEES. As a result, the color of the solution sample clearly changed from pale yellow to orange. It is noted that such large bathochromic shift of absorption features of the DPXT-containing sample upon reaction with 2-CEES, from ~445 to ~576 nm, typically generated a reaction product spectrally separated from the DPXT probe, which virtually enabled optimal excitation wavelength for generating high fluorescence contrast in fluorescence sensing. Additionally, DPXT probe displayed faint blue fluorescence upon excitation and presented a quantum yield less than 0.002. In the presence of 2-CEES, the highly nucleophilic sulphur atom of thiocarbonyl moiety readily underwent nucleophilic reaction with the highly electrophilic sulfonium ion intermediate; this reaction typically triggered ring-opening of the cyclic sulfonium intermediate and transformation of probe into thiopyronin species with a fluorescence quantum yield up to 0.53 because of the change in π-electron delocalization features originating from the transformation of thioketone to thioether form. The combination of huge separation in absorption band and the appreciable increase in fluorescing ability of the probe upon reaction with 2-CEES is expected to generate remarkable beaconing fluorescence contrast for detetcing 2-CEES with high sensitivity.

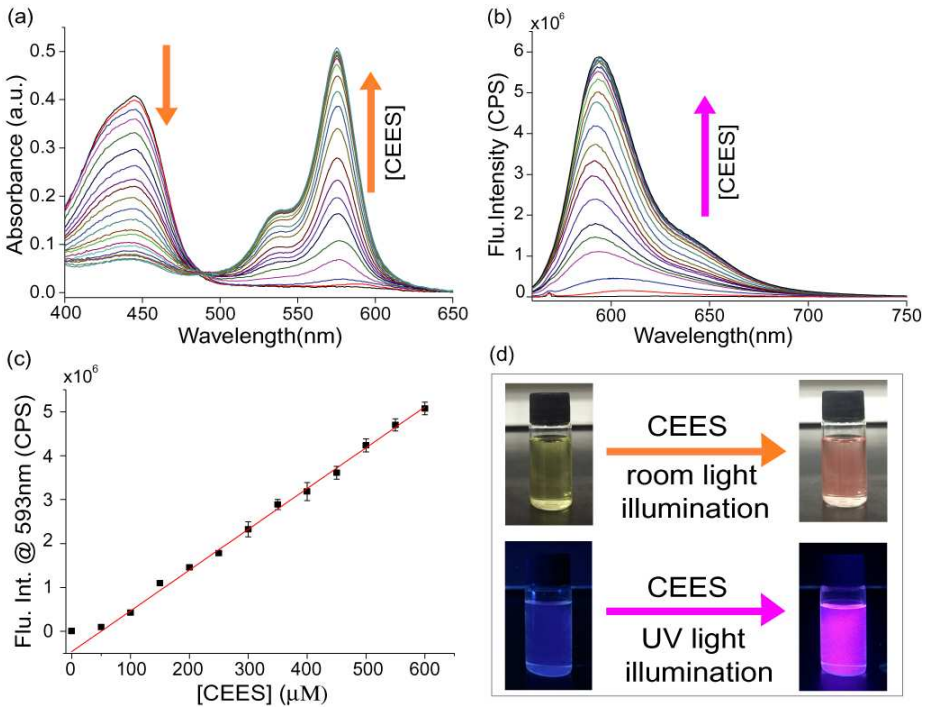

Figure 1. Evolution of UV-vis absorption (a) and fluorescence emission spectra (b) of DPXT/DCM solution upon gradual addition of 2-CEES. (c) A plot of the fluorescence peak intensity (at 593 nm) against the concentration of 2-CEES. The red line is the linear calibration curve with regression coefficient (R^2) of 0.994. (d) Photographs of DPXT/DCM solution before and after addition of 100 equiv. of 2-CEES under room light (top) and UV light (down) illumination. [DPXT] = 10 μM.

The excitation wavelength for acquiring fluorescence spectra of the DPXT/DCM sample in the presence of 2-CEES (Figure 1b) was 570-nm. It can be clearly seen from Figure 1a that such excitation wavelength is not within absorption region of DPXT but very close to the optimum excitation wavelength of the reaction product (~576 nm). Thus, large beaconing signal contrast and high sensitivity to 2-CEES of the probe are expected in fluorescence sensing. Upon excitation at 570 nm, the DPXT/DCM sample without 2-CEES hardly fluoresced, as shown in Figure 1b. In sharp contrast, a new emission band in the range of 580−720 nm with peak at ~

593 nm clearly emerged and gradually augmented upon incremental addition of 2-CEES, eventually generated a solution sample emitting vivid pink fluorescence. Specifically, addition of ~100 equiv. of 2-CEES markedly generated enhancement of the beaconing fluorescence signal (at 593 nm) more than 850-fold. Figure 1c displays the fluorescence titration result of the DPXT probe sample with the aliquots of 2-CEES ranging from 0 to 600 μM. To verify response feature of DPXT probe to 2-CEES with lower concentration range, fluorescence response of DPXT probe to 2-CEES with concentration in range of 0-5μM was investigated. Specifically, perfect linear relationship between the fluorescence signal intensity and the concentration of 2-CEES was obtained (Figure S3), which presented a detection limit of 1.2 μM for 2-CEES sensing. Such sensitivity is equivalent to ~0.6 μM of real SM agent in light of the "half mustard" nature of 2-CEES and about 10 times superior than the counterpart SM sensing ability reported previously,[30,33,35,36,43] indicating the superiority in detection sensitivity of DPXT probe. We noticed that an acridinethione-based SM probe with similar sensing mechanism and a limit of fluorescence detection of ~31.6 μM (0.005mg/mL) was reported very recently,[44] which is more than 52 times coarser than the detection sensitivity that DPXT probe enabled (□0.6 μM). Such superior sensitivity that DPXT probe displayed can be attributed to the sharp contrast between the intrinsic electronic structure features of DPXT molecule and the SM-mediated reaction product (thiopyronin derivative), as discussed in the next section.

Recognition Specificity of DPXT to 2-CEES. To gauge the recognition specificity of DPXT probe to 2-CEES, the fluorescence responses of DPXT/DCM sample to interferent substances with similar reactivities such as acylating agents, alkylating agent, sulphur-containing compounds, and hydrochloric acid were investigated. As illustrated in Figure 2a, fluorescence emission features of the DPXT probe sample nearly remained unchanged in the presence of

various interferent substances as compared to the free DPXT probe sample even if the concentration of these interferent substances largely exceeded that of the probe (200 equiv.). In marked contrast to such almost unresponsive feature, 2-CEES with half concentration of the interferent substances (100 equiv.) clearly induced more than 850-fold augmentation of the beaconing fluorescence signal, unequivocally indicating a high recognition specificity of DPXT for 2-CEES sensing over similarly reactive toxic reagents. As illustrated in Figure 2c,d, DPXT-containing solution samples in the presence of 2-CEES and interfering substances, respectively, clearly presented distinct contrast in both vision and fluorescence mode, suggesting a facile way of monitoring SM using DPXT probe.

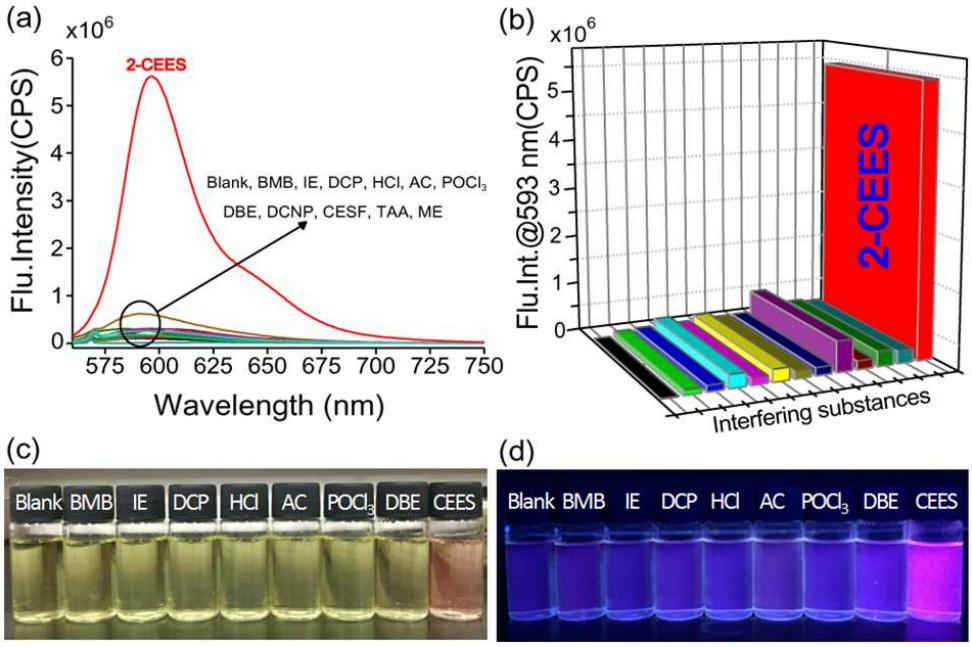

Figure 2. (a) Fluorescence emission spectra of the DPXT/DCM sample (10 μM) with and without of 2-CEES (100 equiv.) and interferent substances (200 equiv.), respectively. (b) Fluorescence peak intensity (at 593nm) of the DPXT/DCM sample in the presence of 2-CEES and various interferent substances. Photographs of DPXT (10 μM) in the absence and presence

of 2-CEES, part typical interferent substances (c) under indoor light and (d) the illumination of a hand-held UV lamp (Ex. 365 nm).

Response of DPXT-loaded Substrate to Gaseous 2-CEES. SM is hazardous to humans in both liquid and vapor form.[26] Thus, one of the key litmus test for SM probes is whether they are capable of detecting SM vapor with concentration at or below the margin of safety (AEGL-1 level), especially for practical detection applications in which warm climates facilitate vaporization of SM[26]. To evaluate the effectiveness of DPXT probe for detecting SM in gas phase, the fluorescence response of DPXT-loaded substrates to gaseous 2-CEES was investigated. In a typical protocol, a DPXT-patterned TLC plate with logo of "CEES" was imaged before and after exposure to 0.5 ppm 2-CEES vapor, respectively. It was found that the DPXT-loaded TLC plates after treatment in vapor presented marked contrast in color and fluorescence brightness to those of the plate prior to 2-CEES vapor treatment (Figure 3a). Specifically, the logo of "CEES" on the patterned TLC plate before exposure to 2-CEES vapor was hardly distinguishable from the DPXT-free part upon illumination of UV light. In sharp contrast, the patterned TLC plate after exposure to 2-CEES vapor clearly presented the logo of "CEES" with very clear edge from the DPXT-free part, fluorecing vivid pink color upon illumination of UV light. Additionally, such DPXT-loaded TLC plate after exposure to 2-CEES vapor presented pink fluorescence ~16 times brighter than that of the plate before exposure to 2-CEES vapor (Supporting Information), indicating the high sensitivity of such DPXT-loaded platform for gaseous SM sensing.

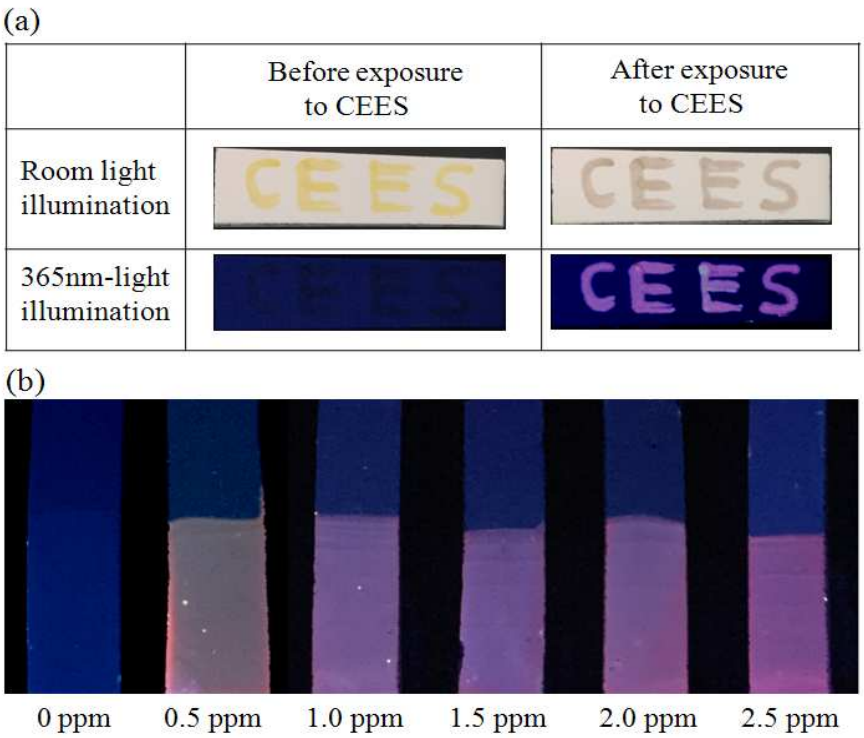

Figure 3. (a) Photographs of a TLC plate patterned with "CEES" using DPXT/DCM solution before and after 1-min exposure to 0.5 ppm 2-CEES vapor acquired via illumination of indoor light and UV lamp, respectively. (b) Photographs of six parallel TLC plates with one end of each loaded with DPXT after exposure to 2-CEES vapor with concentration 0f 0, 0.5, 1.0 1.5, 2.0, 2.5 ppm acquired via illumination of UV light.

To evaluate the sensing limit of DPXT to gaseous SM, six parallel DPXT-loaded TLC plates were prepared via the same procedure and their photographs before and after exposure to gaseous 2-CEES with various concentration were acquired under illumination of 365-nm UV light. Specifically, the concentration of 2-CEES gas in six sealed containers was 0, 0.5, 1.0, 1.5, 2.0, 2.5 ppm, respectively, and the exposure duration was 1 minute in all cases. The TLC plate underwent exposure to atmosphere without 2-CEES gas (0 ppm gas) did not display noticeable boundary line between its DPXT-loaded end and the DPXT-free end, both presenting vivid blue color throughout the whole TLC plate (Figure 3b). In sharp contrast, the DPXT-loaded end of

TLC plate after exposure to 0.5 ppm 2-CEES gas clearly presented pink fluorescence upon illumination of UV light and therefore generated a clear boundary line between the DPXT-loaded end and the DPXT-free end. Upon increasing the concentration of 2-CEES gas that the TLC plates were exposed to, color and brightness contrast between the DPXT-loaded end and the DPXT-free end obviously increased, which is in line with the fluorescence analysis results in the case of solution DPXT probe sample for 2-CEES sensing in its liquid form (Figure 1c). These results indicate that the platform with DPXT immobilized on the TLC plate is capable of reporting the exixtence of 2-CEES gas with concentration down to 0.5 ppm in the case of acute exposure with duration of 1 minute.

It is noted that the lower limit concentration of 2-CEES vapor in the above-mentioned 2-CEES gas sensing experiments was 0.5 ppm, which is equivalent to 0.25 ppm of gaseous SM[11, 34]. Such detection sensitivity to SM, namely 0.25 ppm/min, is much higher than the highest sensitivity regarding SM fluorescence detection reported to date, namely 6.25 ppm/30 min.[36] Wolfbeis et al recently reported enzyme-based platform enabling photographic detection of SM gas with dose schema level down to 4.2 ppm/min (3 μg/L on the basis of 10-min exposure duration),[30] which is a significant progress regarding SM sensing. According to the AEGL-1 safety criterion regarding SM exposure, namely acute exposure at 0.6 ppm/min level, the detection sensitivities of all these probes/sensors reported to date are not sufficient for providing alert signals when the concentration of SM reaches the ceiling level. In marked contrast, the detetcion limit that our DPXT probe enabled (0.25 ppm/min) is indeed below such safety ceiling level, to which individual may be exposed in accidental cases of acute exposure to SM.[15,16] Unequivocally, DPXT probe developed in this work displayed sensing ability for providing timely alert signals before accumulation of SM exerts adverse effects on human health.

Sensing Mechanism. The high sensitivity that DPXT probe exhibited is determined by its unique molecular structure. As discussed above, using sulfur as active site enabled the high reactivity of DPXT probe toward SM species by maximizing it nucleophicility. Moreover, the intrinsic electronic structure feature of thiocarbonyl-containing DPXT molecule endowed limited π-conjugation and therefore high-energy absorption to the probe. On the other hand, SM-mediated nucleophilic reaction of the DPXT probe yielded the thiopyronin derivative with two nitrogen atoms of the piperidyl substituents involved in delocalization of the positive charge from the core heterocyclic framework, which is characterized with absorption and emission features at significantly lower energy regions as compared to other counterpart pyronin derivatives.[45] To shed light on the key role of the piperidyl substituents, we synthesized a reference compound with similar molecular skeleton but without the piperidyl substituents, xanthene-9-thione (XTT), and investigated its optical responses to 2-CEES (Figure S5). In sharp contrast to DPXT, the reference compound XTT after exposure to 2-CEES did not display appreciable absorption in the range of 480-640 nm and therefore can not be excited by 570-nm light. As a result, no appreciable fluorescence enhancement of XTT upon exposure to 2-CEES was observed. Such performance of this reference compound definitely verified the key role of 3, 6-position electron-donating piperidyl moieties in DPXT for enabling the fluorescence response features. The resultant marked difference in the maxima of absorption band, up to 131 nm, virtually enables sufficient spectral separation of the thiopyronin dye from the DPXT probe and therefore optimal excitation wavelength for generating high fluorescence contrast for SM sensing. Additionally, the thiopyronin derivative is generally featured with much higher fluorescence quantum yield (ϕ = 0.53) as compared to that of the DPXT probe (ϕ less than 0.002), which

provides another enabling factor contributing to high fluorescence contrast for SM sensing with high sensitivity.

Conclusions

To conclude, we have developed pyronin-based fluorescent probe, DPXT, capable of detecting SM with limit of detection down to 0.6 μM in solution phase and 0.25 ppm/min SM in gas phase, respectively, which is the first fluorescent probe enabled detecting gaseous SM with concentration indeed below the AEGL-1 level (0.6 ppm/min). Such nearly nonfluorescent DPXT probe readily react with SM via nucleophilic reaction process and therefore yielded highly fluorescent thiopyronin derivative, which yielded distinct contrast in fluorescence emission features between the reaction product and the probe. The excellent recognition specificity of the DPXT probe to SM species was also verified. The proposed sensing mechanism was sufficiently supported by UV-vis absorption and fluorescence emission spectroscopy, NMR, mass spectrum characterization results, as well as the response features of reference compound (Supporting Information). Such unprecedented detection sensitivity and excellent recognition specificity that DPXT probe displayed unequivocally proclaimed its potential for prompt and reliable detection of highly hazardous SM species characterized with latent phase of intoxication in practical applications.

■ ACKNOWLEDGMENTS

This work was financially supported by the National Natural Science Foundation of China (grant no. 21373218 and 21573234) and the Instrument Developing Project of the Chinese Academy of Sciences (Grant YZ201455).

Supporting Information.

Reaction time studies, screening of solvent, partial ^{1}H NMR (400 MHz) spectral changes of DPXT probe in CD_2Cl_2 in the absence and presence of 2-CEES, selected comparison of fluorescent probes for 2-CEES or sulfurs mustard as well as copies of NMR spectra and MALDI-MS.

AUTHOR INFORMATION

Corresponding Author

*E-mail: zytian@ucas.ac.cn; jjh@ucas.ac.cn

Notes

The authors declare no competing financial interest.

■ REFERENCES

(1) Saladi, R.; Smith, E.; Persaud, A. *Clin. Exp. Dermatol.* **2006**, *31*, 1-5.

(2) Shohrati, M.; Davoudi, M.; Ghanei, M.; Peyman, M.; Peyman, A. *Cutan. Ocul. Toxicol.* **2007**, *26*, 73-81.

(3) Szinicz, L. *Toxicol.* **2005**, *214*, 167-181.

(4) Borak, J.; Sidell, F. R. *Ann. Emergency Med.* **1992**, *21*, 303-308.

(5) Fitzgerald, G. J. *Am. J. Public Health* **2008**, *98*, 611-625.

(6) Balali□Mood, M.; Hefazi, M. *Fundam. Clin. Pharmacol.* **2005**, *19*, 297-315.

(7) Kehe, K.; Szinicz, L. *Toxicol.* **2005**, *214*, 198-209.

(8) Davis, K. G.; Aspera, G. *Ann. Emergency Med.* **2001**, *37*, 653-656.

(9) Takeshima, Y.; Inai, K.; Bennett, W. P.; Metcalf, R. A.; Welsh, J. A.; Yonehara, S.; Hayashi, Y.; Fujihara, M.; Yamakido, M.; Akiyama, M. *Carcinogenesis* **1994**, *15*, 2075-2079.

(10) Gilman, A.; Philips, F. S. *Science* **1946**, *103*, 409-436.

(11) Shakarjian, M. P.; Heck, D. E.; Gray, J. P.; Sinko, P. J.; Gordon, M. K.; Casillas, R. P.;

Heindel, N. D.; Gerecke, D. R.; Laskin, D. L.; Laskin, J. D. *Toxicol. Sci.* **2009**, *114*, 5-19.

(12) Patel. V. R.; Parmar, J. N.; Aal, L. B.; Sen, D. J. *Int J Pharm Res Sci.,* **2014**, 3, 332-357.

(13) Mellor, S.; Rice, P.; Cooper, G. *Br. J. Plast. Surg.* **1991**, *44*, 434-437.

(14) Pathak, U.; Raza, S. K.; Kulkarni, A.; Vijayaraghvan, R.; Kumar, P.; Jaiswal, D. K. *J. Med. Chem.* **2004**, *47*, 3817-3822.

(15) Wattana, M.; Bey, T. *Prehosp. Disaster Med.* **2009**, *24*, 19-29.

(16) Watson, A.; Opresko, D.; Young, R.; Hauschild, V. *J. Toxicol. Environ. Health, Pt. B Crit. Rev.* **2006**, *9*, 173-263.

(17) Black, R. M.; Clarke, R. J.; Cooper, D. B.; Read, R. W.; Utley, D. *J. Chromatogr. A* **1993**, *637*, 71-80.

(18) D'Agostino, P.; Provost, L. R. *J. Chromatogr. A* **1992**, *600*, 267-272.

(19) Kientz, C. E. *J. Chromatogr. A* **1998**, *814*, 1-23.

(20) Wils, E.; Hulst, A.; De Jong, A. *J. Chromatogr. A* **1992**, *625*, 382-386.

(21) Black, R. M.; Read, R. W. *J. Chromatogr. A* **1991**, *558*, 393-404.

(22) Jakubowski, E.; Woodard, C.; Mershon, M.; Dolzine, T. *J. Chromatogr. B Biomed. Appl.* **1990**, *528*, 184-190.

(23) Baruah, M.; Qin, W.; Vallée, R. A.; Beljonne, D.; Rohand, T.; Dehaen, W.; Boens, N. *Org. Lett.* **2005**, *7*, 4377-4380.

(24) Baumbach, J. I.; Eiceman, G. A. *Appl. Spectrosc.* **1999**, *53*, 338A-355A.

(25) Bunkar, R.; Vyas, K.; Rao, V.; Kumar, S.; Singh, B.; Kaushik, M. *Sens. Transducers J.* **2010**, *113*, 41-47.

(26) Boopathi, M.; Suryanarayana, M.; Nigam, A. K.; Pandey, P.; Ganesan, K.; Singh, B.; Sekhar, K. *Biosens. Bioelectron.* **2006**, *21*, 2339-2344.

(27) Wang, Q.-Q.; Ara Begum, R.; Day, V. W.; Bowman-James, K. *Inorg. Chem.* **2011**, *51*, 760-762.

(28) Gp, V. D. S.; Scheffer, A. G.; Marsgroenendijk, R. H.; Fidder, A.; Benschop, H. P.; Baan, R. A. *Chem. Res. Toxicol.* **1994**, *7*, 408.

(29) Van-Der-Schans, G.; Noort, D.; Mars-Groenendijk, R.; Fidder, A.; Chau, L.; De-Jong-Leop, A.; Benschop, H. *Chem. Res. Toxicol.* **2002**, *15*, 21-25.

(30) Bidmanova, S.; Steiner, M.-S.; Stepan, M.; Vymazalova, K.; Gruber, M. A.; Duerkop, A.; Damborsky, J.; Prokop, Z.; Wolfbeis, O. S. *Anal. Chem.* **2016**, *88*, 6044-6049.

(31) Sun, W.; Guo, S. G.; Hu, C.; Fan, J. L.; Peng, X. J. *Chem. Rev.* **2016**, 116, 7768-7817.

(32) Liu, H. W.; Liu, Y. C.; Wang, P.; Zhang, X. B. Methods Appl. Fluoresc. **2017**, 5, 012003.

(33) Kumar, V.; Anslyn, E. V. *J. Am. Chem. Soc.* **2013**, *135*, 6338-6344.

(34) Brookes, P.; Lawley, P. *Biochem. J* **1961**, *80*, 496.

(35) Kumar, V.; Anslyn, E. V. *Chem. Sci.* **2013**, *4*, 4292-4297.

(36) Goud, D. R.; Purohit, A. K.; Tak, V.; Dubey, D. K.; Kumar, P.; Pardasani, D. *Chem. Commun.* **2014**, *50*, 12363-12366.

(37) Zhang, Y. L.; Peng A. D.; Jie, X. K.; Lv, Y. L.; Wang, X. F.; Tian, Z. Y. *ACS Appl. Mater. Interfacses* **2017**, *9*, 13920-13927.

(38) Fava, A.; Reichenbach, G.; Peron, U. *J. Am. Chem. Soc.* **1967**, *89*, 6696-6700.

(39) Saygılı, N.; Saygıl, Nezire. *Hacettepe Univ. J. Fac. Pharm.,* **2011**, 31,15-26.

(40) Demas, J. *J. Phys. Chem.* **1971**, *75*, 991-1024.

(41) Arbeloa, F. L.; Ojeda, P. R.; Arbeloa, I. L. *J. Lumin.* **1989**, *44*, 105-112.

(42) Long, G. L.; Winefordner, J. D. *Anal. Chem.* **1983**, *55*, 712A-724A.

(43) Kumar, V.; Rana, H. *RSC Advances* **2015**, *5*, 91946-91950.

(44) Kumar, V.; Rana, H.; Raviraju, G.; Gupta, A. K. *Anal. Chem.* **2018**, 90, 1417-1422.

(45) Wu, L.; Burgess, K. *Org. Lett.* **2008**, *10*, 1779-1782.

Table of Contents

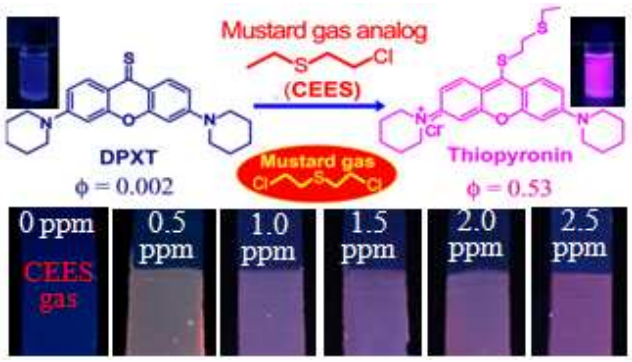

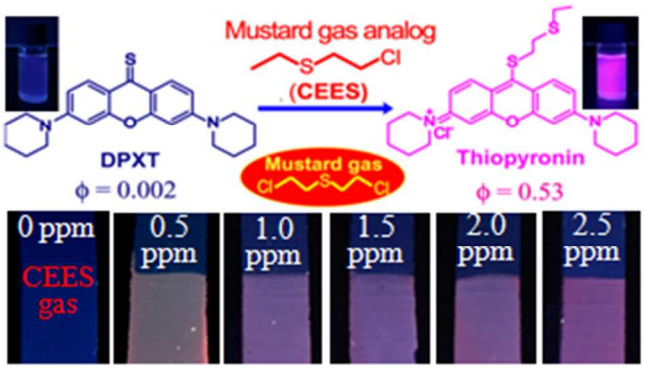

Table of Contents

115x64mm (72 x 72 DPI)